Article

Nonlinear Optical Studies of the Agricultural Antibiotic Morantel Interacting with Silica/Water Interfaces

Christopher T. Konek, Kimberly D. Illg, Hind A. Al-Abadleh, Andrea B. Voges, Grace Yin, Michael J. Musorrafiti, Catherine M. Schmidt, and Franz M. Geiger

J. Am. Chem. Soc., **2005**, 127 (45), 15771-15777• DOI: 10.1021/ja054837b • Publication Date (Web): 19 October 2005

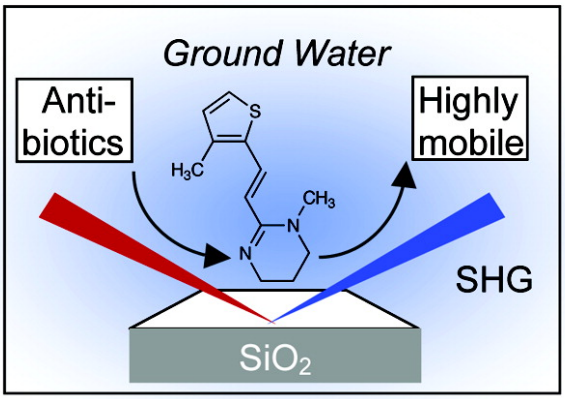

More About This Article

Additional resources and features associated with this article are available within the HTML version:

- Supporting Information
- Links to the 6 articles that cite this article, as of the time of this article download
- Access to high resolution figures
- Links to articles and content related to this article
- Copyright permission to reproduce figures and/or text from this article

View the Full Text HTML

J|A|C|S
ARTICLES
Published on Web 10/19/2005

Nonlinear Optical Studies of the Agricultural Antibiotic Morantel Interacting with Silica/Water Interfaces

Christopher T. Konek, Kimberly D. Illg, Hind A. Al-Abadleh,[#] Andrea B. Voges, Grace Yin, Michael J. Musorrafiti, Catherine M. Schmidt, and Franz M. Geiger*

Contribution from the Department of Chemistry and the Institute for Environmental Catalysis, Northwestern University, 2145 Sheridan Road, Evanston, Illinois 60208

Received July 19, 2005; E-mail: geigerf@chem.northwestern.edu

Abstract: It is now known that the untreated discharge of pharmaceuticals into the environment can impact human health and development and lead to increased drug resistance in biota. Here, we present the first direct interface-specific studies that address the mobility of the widely used agricultural antibiotic morantel, which is commonly present in farm runoff. Surface-bound morantel was spectroscopically identified using second harmonic generation (SHG) via a two-photon resonance of its n$-\pi^*$ transition and in the C$-$H stretching region by vibrational sum frequency generation (VSFG). Resonantly enhanced SHG adsorption isotherm measurements carried out at the silica/water interface between 6×10^{-7} and 5×10^{-5} M morantel concentration result in a free energy of adsorption of 42(2) kJ/mol at pH 7. Finally, real-time tracking of morantel interaction with the silica/water interface shows that the binding events are fully reversible, consistent with its high mobility in silica-rich soil environments. This work thus indicates that pharmaceuticals discharged into the environment can enter the groundwater supply of municipal water systems, at which point their removal is challenging. In addition, the high mobility of morantel in silica-rich soil environments could lead to developing increased interaction of this antibiotic with target organisms, which could respond by increased drug resistance.

I. Introduction

The release of agricultural antibiotics and chemicals into the environment has received much attention recently.[1−9] It is estimated that 70% of all antibiotic use in the United States occurs on animal farms,[10] much of which is nontherapeutic to promote growth. Discharges of veterinary antibiotics can lead to increased drug resistance in biota.[5,6] In recognition of this problem, the FDA recently banned the use of the veterinary antibiotic Baytril, which is used on poultry farms.[11] A related concern is the release of herbicides and pesticides as well as hormones, which can act as environmental endocrine disruptors and potentially result in the premature onset of puberty, decreased fertility in males, gonadal abnormalities, and Creutzfeldt-Jakob-like diseases.[1−4] Given the increase in agribusiness over the past 50 years[12] and increased stresses on freshwater supplies,[13] these issues represent a major emerging problem for chemistry, biology, and engineering. As with toxic metals, the bioavailability of agricultural chemicals is in a large part determined by the transport of these species through soil environments.[14−17] The transport properties, in turn, can be controlled by heterogeneous processes occurring at mineral/water interfaces, such as adsorption and desorption.[18,19] Tracking these processes directly at environmental interfaces and under environmentally representative concentrations represents a major challenge in geochemistry.

In this work, we present the first nonlinear optical studies that examine how morantel, a widely used agricultural antibiotic, interacts with a prototypical mineral/water interface. Morantel

[#] Present address: Wilfred Laurier University, Waterloo, Canada.

(1) Howdeshell, K. L.; Hotchkiss, A. K.; Thayer, K. A.; Vandernberg, J. G.; vom Saal, F. S. *Nature* **1999**, *401*, 763.
(2) Anway, M. D.; Cupp, A. S.; Uzumcu, M.; Skinner, M. K. *Science* **2005**, *308*, 1466.
(3) Hayes, T.; Haston, K.; Tsui, M.; Hoang, A.; Haeffele, C.; Conk, A. *Nature* **2002**, *419*, 895.
(4) Aguzzi, A.; Montrasio, F.; Kaeser, P. S. *Nat. Rev. Mol. Cell Biol.* **2001**, *2*, 118.
(5) Ferber, D. *Science* **2000**, *288*, 792.
(6) Molbak, K.; Baggesen, D. L.; Aarestrup, F. M.; Ebbesen, J. M.; Engberg, J.; Frydendahl, K.; Gerner-Smidt, P.; Petersen, A. M.; Wegener, H. C. *N. Engl. J. Med.* **1999**, *341*, 1420.
(7) Stackelberg, P. E.; Furlong, E. T.; Meyer, M. T.; Zaugg, S. D.; Henderson, A. K.; Reissman, D. B. *Sci. Total Environ.* **2004**, *329*, 99.
(8) Jones, O. A.; Lester, J. N.; Vouvoulis, N. *Trends Biotechnol.* **2005**, *23*, 163.
(9) Kolpin, D. W.; Furlong, E. T.; Meyer, M. T.; Thurman, E. M.; Zaugg, S. D.; Barber, L. B.; Buxton, H. T. *Environ. Sci. Technol.* **2002**, *36*, 1202.
(10) Mellon, M.; Benbrook, C.; Benbrook, K. L. *Hogging It: Estimates of Antimicrobial Abuse in Livestock*; Union of Concerned Scientists: Cambridge, MA, 2001.
(11) Hileman, B. *Chem. Eng. News* **2005**, *83*, 16.
(12) Matson, P. A.; Parton, W. J.; Power, A. G.; Swift, M. J. *Science* **1997**, *277*, 504.
(13) Vorosmarty, C. J.; Green, P.; Salisbury, J.; Lammers, R. B. *Science* **2000**, *289*, 284.
(14) Evangelou, V. P. *Environmental Soil and Water Chemistry*; John Wiley & Sons: New York, 1998.
(15) Stumm, W.; Morgan, J. J. *Aquatic Chemistry*, 3rd ed.; Wiley-Interscience: New York, 1996.
(16) Morel, F. M. M.; Hering, J. G. *Principles and Applications of Aquatic Chemistry*; Wiley-Interscience: New York, 1993.
(17) Schwarzenbach, R. P.; Gschwend, P. M.; Imboden, D. M. *Environmental Organic Chemistry*, 2nd ed.; John Wiley and Sons: Hoboken, NJ, 2003.
(18) Brown, G. E. *Science* **2001**, *294*, 67.
(19) Brown, G. E.; Henrich, V. E.; Casey, W. H.; Clark, D. L.; Eggleston, C.; Felmy, A.; Goodman, D. W.; Graetzel, M.; Maciel, G.; McCarthy, M. I.; Nealson, K. H.; Sverjensky, D. A.; Toney, M. F.; Zachara, J. M. *Chem. Rev.* **1999**, *99*, 77.

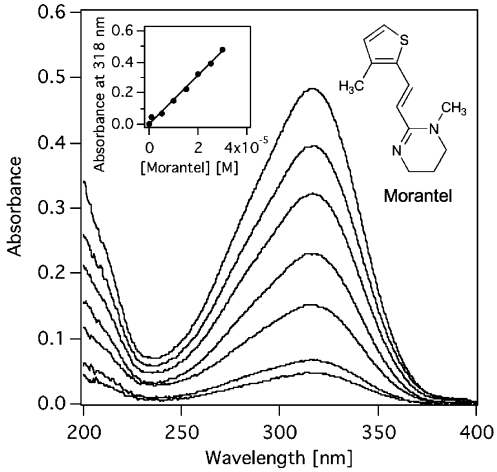

Figure 1. UV−vis spectra of morantel at pH 7 and increasing morantel concentration. Inset: Absorbance at 318 nm as a function of morantel concentration.

(1,4,5,6-tetrahydro-1-methyl-2(2-(3-methyl-2-thienyl)ethenyl)-pyrimidine, see Figure 1) is a member of the tetrahydropyrimidine group that is used in the cattle industry as an antinematodal, or deworming, antibiotic.[20] Morantel is readily soluble in water[21] and has a high potential for entering the environment.[22] The interaction of this antihelmintic with acetylcholine receptors of the parasites is used to control and remove mature gastrointestinal nematode infections in cattle and goats.[20] It has been available in the United States since 1982, with average dosing levels of 4.4 mg/lb body weight of the animal.[20] Only about one-quarter of this amount is metabolized by the animal, with the remainder being excreted essentially unchanged.[23] However, morantel residue concentrations of 84 and 170 ng/mL have been reported in dairy cattle milk and plasma, respectively.[24] As a consequence, morantel is subject to the USDA's Food Safety and Inspection Service National Residue Program,[25] the analytical testing program for residues in domestic and imported meat, which lists the lowest detectable limit (LDL) in cattle liver at 0.25 ppm.[26]

In the United States, it has been estimated that on average 6600 kg of morantel is introduced into the environment every year,[20] where its presence could lead to morantel resistance in nematodes and other biota. While resistance to morantel has not yet been reported, assessing its mobility provides important information on the likelihood of morantel resistance in the target biota; if morantel were highly mobile in soils, and if it were discharged into the environment from farms on a daily basis (i.e., constant flux), the contact frequency between this drug and its target would clearly be higher than in the case of immobile morantel. Assessing the mobility of morantel in soils thus provides a first step toward understanding the risks associated with drug resistance development in biota. Due to rapid dilution, this concern would clearly decrease with increasing distance away from the farms. However, given the possibility for the development of drug resistance in parasites exposed to morantel present in farm runoff, determining the mobility of morantel in the environment is necessary in order to assess its potential for leaching into the groundwater and its subsequent environmental fate.

In contrast to inorganic metal contaminants and many halogenated organic compounds, surprisingly little is known about the environmental fate of veterinary pharmaceuticals[27] and their molecular-level interactions with mineral/water interfaces. This work seeks to fill this void while addressing important fundamental problems in studying environmental interfaces from a molecular perspective. While chemical binding and surface speciation in soils are generally governed by mechanisms operating at interfaces, chemical transport models commonly rely on pollutant-to-soil binding constants that are derived from bulk measurements.[22,28−31] Specifically, the K_d parameter is widely used to predict contaminant transport in the form of retardation factors,[29,30] but the bulk measurements frequently used for obtaining K_d parameters from the initial slope of adsorption isotherms can overlook important molecular-level processes which may control binding events.[32] Retardation factors derived from interface-specific binding studies may lead to improved predictions of contaminant transport in soils.[32] However, surface-specific approaches are complicated by the fact that many experimental techniques used for studying liquid/solid interfaces are limited by long signal integration times and low surface sensitivities.[19] This is especially important when considering the nonlinear relationship between aqueous phase concentration and surface coverage[15,31,33−35] for small aqueous phase concentrations,[33,34] which makes the extrapolation of data obtained with high bulk concentrations to environmentally representative concentrations problematic. XAFS techniques (XANES and EXAFS) are extremely useful for identifying and characterizing metal-containing adsorbates.[19,36−42] However, organic compounds are difficult to characterize, and even with

(20) Environmental Impact Statement. Pfizer Incorporated: New York, 1994.
(21) *Clarke's Analysis of Drugs and Poisons*, 3rd ed.; Pharmaceutical Press: London, 2003.
(22) Boxall, A. B. A.; Kolpin, D. W.; Halling-Sorensen, B.; Tolls, J. *Environ. Sci. Technol. A-Pages* **2003**, 286.
(23) Melancon, J. J. *A Review of Morantel Citrate*; Merial, 2001, 2005.
(24) Lynch, M. J. M.; Burnett, D. M.; Newby, T. J. *J. Agric. Food Chem.* **1987**, *35*, 351.
(25) 2000 FSIS National Residue Program − The "Blue Book"; Food Safety and Inspection Service, USDA, 2000; http://www.fsis.usda.gov/OPHS/blue2000/.
(26) *Morantel And Pyrantel Drug-Related Metabolites*; US Department of Agriculture Food Saftey and Inspection Service: Athens, GA, 1991.
(27) Schmitt, H.; van Beelen, P.; Tolls, J.; van Leeuwen, C. L. *Environ. Sci. Technol.* **2004**, *38*, 1148.
(28) Tolls, J. *Environ. Sci. Technol.* **2001**, *35*, 3397.
(29) *Understanding Variation in Partition Coefficient, K_d, Values: Introduction*; United States Environmental Protection Agency, 2003; www.epa.gov/radiation/cleanup/partition.htm.
(30) *Understanding Variation in Partition Coefficient, K_d, Values: Appendix E, Partition Coefficients for Chromium (VI)*; United States Environmental Protection Agency, 2003; www.epa.gov/radiation/cleanup/partition.htm.
(31) Langmuir, D. *Aqueous Environmental Geochemistry*; Prentice-Hall: New Jersey, 1997.
(32) Al-Abadleh, H. A.; Mifflin, A. L.; Bertin, P. A.; Nguyen, S. T.; Geiger, F. M. *J. Phys. Chem. B.* **2005**, *109*, 9691.
(33) Sposito, G. *The Surface Chemistry of Soils*; Oxford University Press: New York, 1984.
(34) Adamson, A. W. *Physical Chemistry of Surfaces*, 5th ed.; John Wiley & Sons: New York, 1990.
(35) Masel, R. I. *Principles of Adsorption and Reaction on Solid Surfaces*; John Wiley & Sons: New York, 1996.
(36) Bostick, B. C.; Fendorf, S.; Manning, B. A. *Geochim. Cosmochim. Acta* **2003**, *67*, 895.
(37) Farquhar, M. L.; Charnock, J. M.; Livens, F. R.; Vaughan, D. J. *Environ. Sci. Technol.* **2002**, *36*, 1757.
(38) Foster, A. L.; Brown, G. E.; Parks, G. A. *Geochim. Cosmochim. Acta* **2003**, *67*, 1937.
(39) Paktunc, D.; Foster, A.; Laflamme, G. *Environ. Sci. Technol.* **2003**, *37*, 2067.
(40) Smith, P. G.; Koch, I.; Gordon, R. A.; Mandoli, D. F.; Chapman, B. D.; Reimer, K. J. *Environ. Sci. Technol.* **2005**, *39*, 248.
(41) Takahashi, Y.; Ohtaku, N.; Mitsunobu, S.; Yuita, K.; Nomura, M. *Anal. Sci.* **2003**, *19*, 891.
(42) Weckhuysen, B. M.; Wachs, I. E.; Schoonheydt, R. A. *Chem. Rev.* **1996**, *96*, 3327.

metals, sensitivity issues can make the experiments challenging and real-time measurements of solute−surface binding processes difficult.[42]

Nonlinear optical spectroscopies, specifically, second harmonic generation (SHG) and vibrational sum frequency generation (VSFG), are promising new real-time probes for studying environmentally relevant surfaces and buried interfaces.[32,43−59] They yield not only important spectroscopic and structural information with surface and molecular specificity but also the thermodynamic and kinetic parameters that are vitally needed for obtaining reliable retardation factors. Information derived from such interface-specific data may also aid in understanding the discrepancies between octanol−water partition coefficients and organic−carbon sorption coefficients of a wide range of veterinary pharmaceuticals.[28] By applying SHG and VSFG, surface-bound morantel was spectroscopically identified. SHG was then used to track the interaction of morantel with fused quartz/water interfaces at environmentally representative concentrations. Morantel was found to be highly mobile in silica-rich soil environments. This work clearly demonstrates the capabilities of nonlinear optical spectroscopies to study the mobility of veterinary and agricultural antibiotics, an area not previously explored with nonlinear optics.

II. Experimental Section

1. Surface SHG and SFG: Morantel exhibits electronic transitions in the UV−vis spectral regions that are centered at 285 and 318 nm (Figure 1). The lower energy transition can be attributed to an n→π^* transition of the tetrahydropyrimidine moiety, which, similarly to pyrimidones,[60] exhibits electronic resonances near 320 nm.[61] At a pH of 7, the extinction coefficient at 318 nm was measured to be 15.8(3) $\times$ 10^3 cm^{-1} M^{-1} (Figure 1, inset). Adsorbates with such electronic resonances can be studied using SHG.[53,56,62−66]

The recorded SHG intensity, I_{SHG}, is related to the second-order susceptibility of the interface, $\chi^{(2)}_{int}$.[53,62,66] When the SHG *E*-field, E_{SHG}, is resonantly enhanced, as in the case of adsorbed morantel, $\chi^{(2)}_{int}$ consists of a nonresonant and a resonant contribution, $\chi^{(2)}_{NR}$ and $\chi^{(2)}_{R}$, respectively, which are linked by the difference in their respective phases, $\Delta\phi$, as shown in eq 1:

$$\sqrt{I_{SHG}} = E_{SHG} \propto \sqrt{|\chi^{(2)}_{NR} + \chi^{(2)}_{R} e^{i\Delta\phi}|^2} \tag{1}$$

The resonant contribution to the second-order susceptibility, $\chi^{(2)}_{R}$, can be modeled as the product of the number of adsorbates at the interface, *N*, and the molecular hyperpolarizability, $\alpha^{(2)}$, averaged over all molecular orientations, according to eq 2:

$$\chi^{(2)}_{R} = N\left\langle \overleftrightarrow{\alpha}^{(2)} \right\rangle \tag{2}$$

Equations 1 and 2 show that by monitoring the concentration dependence of the SHG *E*-field one can perform adsorption isotherm measurements. Typically, for resonance-enhanced SHG experiments, the phase difference, $\Delta\phi$, is taken to be 90°, even though other angles down to 0° are, in principle, possible as well.[32,66,67] Similar to the NMR chemical shift tensor, the tensor properties of the molecular hyperpolarizability contain orientational information that can be accessed by using polarization-resolved SHG measurements.[68−70]

For spectroscopic measurements at interfaces, $\alpha^{(2)}$ contains electronic transitions given by electric dipole transition moments, $\vec{\mu}_i$, and ground, intermediate, and final states, a, b, and c, respectively:

$$\left\langle \overleftrightarrow{\alpha}^{(2)}_{ijk} \right\rangle = -\frac{4\pi^2 e^3}{h^2} \sum_{b,c} \frac{\langle a|\vec{\mu}_i|b\rangle\langle b|\vec{\mu}_j|c\rangle\langle c|\vec{\mu}_k|a\rangle}{(\omega - \omega_{ba} - i\Gamma_{ba})(2\omega - \omega_{ca} - i\Gamma_{ca}) + \cdots} \tag{3}$$

The summation is taken over excited states, *e* is the charge of the electron, *h* is Planck's constant, and Γ represents damping coefficients.[56,62,71] In the case of a two-photon resonance, the SHG efficiency increases as 2ω approaches a resonance frequency ω_{ca} in the adsorbate, which allows for interface-specific spectroscopic studies in the UV−vis.

SFG can be viewed as the vibrational analogue of SHG, in which electronic transitions are typically probed.[53,56,62,63,71−77] The complete vibrational spectrum for an interface and its adsorbates can be acquired by scanning the frequency of the incoming IR beam across the vibrational frequencies of the adsorbates or the interface. Compared to scanning SFG experiments, IR fields that are broad in the frequency domain, such as those produced by the femtosecond infrared system employed in this work, allow for the collection of SFG spectra within a single laser pulse. The spectral resolution is chiefly determined by the bandwidth of the visible pump pulse and, to a smaller extent, the monochromator and detector resolutions.[76] Pioneered as broadband sum frequency generation (BBSFG) by vanderHam et al.[77] and Richter et

(43) Stack, A. G.; Higgins, S. R.; Eggleston, C. M. *Geochim. Cosmochim. Acta* **2001**, *65*, 3055.
(44) Fitts, J. P.; Shang, X.; Flynn, G. W.; Heinz, T. F.; Eisenthal, K. B. *J. Phys. Chem. B* **2005**, *109*, 7981.
(45) Liu, D. F.; Ma, G.; Allen, H. C. *Environ. Sci. Technol.* **2005**, *39*, 2025.
(46) Yan, E. C. Y.; Eisenthal, K. B. *J. Phys. Chem. B* **1999**, *103*, 6056.
(47) Liu, Y.; Dadap, J. I.; Zimdars, D.; Eisenthal, K. B. *J. Phys. Chem. B* **1999**, *103*, 2480.
(48) Baldelli, S.; Schnitzer, C.; Campbell, D. J.; Shultz, M. J. *J. Phys. Chem. B* **1999**, *103*, 2789.
(49) Allen, H. C.; Gragson, D. E.; Richmond, G. L. *J. Phys. Chem. B* **1999**, *103*, 660.
(50) Wei, X.; Miranda, P. B.; Shen, Y. R. *Phys. Rev. Lett.* **2001**, *86*, 1554.
(51) Steel, W. H.; Damkaci, F.; Nolan, R.; Walker, R. A. *J. Am. Chem. Soc.* **2002**, *124*, 4824.
(52) Walker, R. A.; Gruetzmacher, J. A.; Richmond, G. L. *J. Am. Chem. Soc.* **1998**, *120*, 6991.
(53) Eisenthal, K. B. *Chem. Rev.* **1996**, *96*, 1343.
(54) Zhang, X.; Esenturk, O.; Walker, R. A. *J. Am. Chem. Soc.* **2001**, *123*, 10768.
(55) Konek, C. T.; Musorrafiti, M. J.; Al-Abadleh, H. A.; Bertin, P. A.; Nguyen, S. T.; Geiger, F. M. *J. Am. Chem. Soc.* **2004**, *126*, 11754.
(56) Voges, A. B.; Al-Abadleh, H. A.; Geiger, F. M. Development of Nonlinear Optical Spectroscopies for Studying Heterogeneous Environmental Catalytic Processes. In *Environmental Catalysis*; Grassian, V. H., Ed.; CRC Press: Boca Raton, FL, 2005.
(57) Mifflin, A. L.; Gerth, K. A.; Weiss, B. M.; Geiger, F. M. *J. Phys. Chem. A* **2003**, *107*, 6212.
(58) Mifflin, A. L.; Gerth, K. A.; Geiger, F. M. *J. Phys. Chem. A* **2003**, *107*, 9620.
(59) Al-Abadleh, H. A.; Voges, A. B.; Bertin, P. A.; Nguyen, S. T.; Geiger, F. M. *J. Am. Chem. Soc.* **2004**, *126*, 11126.
(60) Uray, G.; Verdino, P.; Belaj, F.; Kappe, C. O.; Fabian, W. M. F. *J. Org. Chem.* **2001**, *66*, 6685.
(61) Jug, K.; Hahn, G. *J. Comput. Chem.* **1983**, *4*, 410.
(62) Shen, Y. R. *The Principles of Nonlinear Optics*; John Wiley & Sons: New York, 1984.
(63) Shen, Y. R. *Nature* **1989**, *337*, 519.
(64) Shen, Y. R. *Surf. Sci.* **1994**, *299−300*, 551.
(65) Eisenthal, K. B. Equilibrium and Dynamic Processes at Interfaces by Second Harmonic and Sum Frequency Generation. In *Annual Review of Physical Chemistry*; Strauss, H. L., Babcock, G. T., Leone, S. R., Eds.; Annual Reviews Inc: Palo Alto, CA, 1992; Vol. 43, p 627.
(66) Heinz, T. F. *Nonlinear Surface Electromagnetic Phenomena*; Elsevier Publishers: Dordrecht, The Netherlands, 1991.
(67) Al-Abadleh, H. A.; Mifflin, A. L.; Musorrafiti, M. J.; Geiger, F. M. *J. Phys. Chem. B.* **2005**, *109*, 16852.
(68) Simpson, G. J.; Rowlen, K. L. *Anal. Chem.* **2000**, *72*, 3399.
(69) Simpson, G. J.; Rowlen, K. L. *Anal. Chem.* **2000**, *72*, 3407.
(70) Simpson, G. J.; Westerbuhr, S. G.; Rowlen, K. L. *Anal. Chem.* **2000**, *72*, 887.
(71) Boyd, R. W. *Nonlinear Optics*; Academic Press: New York, 1992.
(72) Miranda, P. B.; Shen, Y. R. *J. Phys. Chem. B* **1999**, *103*, 3292.
(73) Richmond, G. L. *Chem. Rev.* **2002**, *102*, 2693.
(74) Buck, M.; Himmelhaus, M. *J. Vac. Sci. Technol. A-Vac. Surf. Films* **2001**, *19*, 2717.
(75) Wei, X.; Hong, S. C.; Lvovsky, A. I.; Held, H.; Shen, Y. R. *J. Phys. Chem. B* **2000**, *104*, 3349.
(76) Richter, L. J.; Petralli-Mallow, T. P.; Stephenson, J. C. *Opt. Lett.* **1998**, *23*, 1594.
(77) vanderHam, E. W. M.; Vrehen, Q. H. F.; Eliel, E. R. *Surf. Sci.* **1996**, *368*, 96.

al.,[76] this technique can lead to short collection times as a step toward real-time monitoring of in situ reactions and dynamics.[76,78] The intensity of the SFG signal, I_{SFG}, is directly proportional to the square modulus of the second-order susceptibility of the interface, $\chi^{(2)}$, which, just as in SHG, can be broken down into a nonresonant contribution and a resonant contribution, $\chi^{(2)}_{NR}$ and $\chi^{(2)}_{R\nu}$, respectively:[79]

$$I_{SFG} \propto |\chi^{(2)}_{NR} + \sum_{\nu=1}^{n} \chi^{(2)}_{R\nu} e^{i\gamma_\nu}|^2 \quad (4)$$

The resonant second-order susceptibility contains resonant contributions from each vibrational mode, ν, and the contributions from the n vibrational modes are coupled by their relative phases, γ_ν. Similar to SHG, the resonant contribution to the second-order susceptibility is proportional to the number of adsorbates and the orientationally averaged molecular hyperpolarizability, which in the case of SFG spectroscopy is commonly named β_ν.[62] When the frequency of the incoming IR beam is in resonance with a vibrational transition of the adsorbate or interface, β_ν increases according to eq 5:[79]

$$\beta_\nu = \frac{A_{\nu,ij} M_{\nu,k}}{\omega_{IR} - \omega_\nu - i\Gamma_\nu} \quad (5)$$

For a given mode ν, A_ν is the Raman transition probability, M_ν is the infrared transition dipole moment, i, j, and k refer to the surface coordinate system, ω_ν is the infrared frequency of the vibrational mode in the surface-bound species, and ω_{IR} is the frequency of the infrared probe light. The damping coefficient Γ_ν avoids singularities and is related to the natural line width of the infrared resonance at frequency ν. Equation 5, coupled with eq 4, shows that resonance enhancement of β_ν leads to resonant enhancement of $\chi^{(2)}_{R\nu}$ and thus of the SFG signal intensity. In general, the nonresonant contributions to the SFG signal for hydrocarbons on insulator surfaces are small.[80]

2. Laser and Detection System: The laser system consists of a regeneratively amplified Ti:sapphire laser system (1 kHz, 120 fs, 1mJ/pulse, Hurricane, Spectra Physics) pumping two optical parametric amplifiers each containing a β-barium borate (BBO) crystal for signal and idler generation (OPA-CF, Spectra Physics). The system has been described in detail previously.[32,56−59,67,81] Briefly, each BBO crystal generates a signal beam between 1.1 and 1.6 μm and an idler beam between 1.6 and 2.6 μm. For the SHG measurements, the frequency-doubled signal from the first OPA, ranging between 560 and 710 nm, was focused onto the aqueous/solid interfaces at an angle of 60° and a spot size approximately 50 μm in diameter and was used to monitor the adsorbates via their two-photon resonances (vide infra). After isolating the SHG signal via Schott filters and a monochromator, the SHG signal was collected using a single-photon counting system. The quadratic power dependence of the SHG signal and its proper spectral response was verified.

For the SFG studies, the second OPA was used to mix the signal and idler beams in a $AgGaS_2$ crystal to produce broadband infrared radiation at a center frequency near 2900 cm^{-1} (bandwidth ~140 cm^{-1}) and with a pulse length of 120 fs and a kilohertz repetition rate. The infrared and the visible upconverter (800 nm) light fields are overlapped in space and time at the surface of interest after decreasing the upconverter bandwidth to about 1.6 nm using a narrow band-pass filter. The SFG studies were carried out using the ssp polarization combination, in which the s-polarized component of the SFG signal is detected while probing with p-polarized infrared light and upconverting with s-polarized 800 nm light. The optical light fields are incident and exigent from the airside of a glass slide that had been submersed in an aqueous 5.6×10^{-5} M morantel solution for 7 min and then air-dried. This concentration corresponds to morantel monolayer coverage (vide infra). After isolating the SFG signal by spatial and optical filtering, the polarization of the SFG signal was rotated for optimal throughput in a 0.5 m spectrograph prior to detecting the dispersed broadband SFG signal using a liquid nitrogen-cooled, back-thinned charged coupled device. Poly(methyl methacrylate) (PMMA) on glass provided a spectral reference.[81] The reproducibility of the absolute SFG peak position is ±5 cm^{-1}, and the spectral resolution of the experiments is ~20 cm^{-1}.[81]

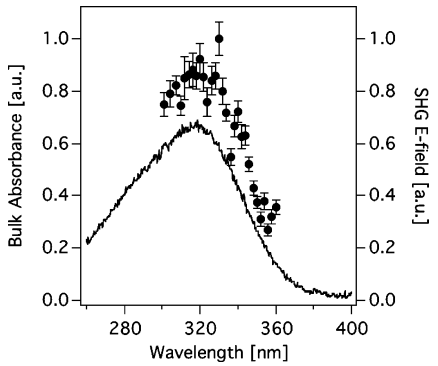

Figure 2. SHG spectrum of morantel adsorbed at the silica/water interface maintained at pH 7 (filled circles, right axis) and bulk UV−vis spectrum at the same pH (solid line, left axis).

3. Sample Cell and Flow System: Since silicates are commonly found in the inorganic soil phase,[14,31] we have chosen the fused quartz/water interface as an initial heterogeneous system for our studies. Naturally occurring quartz is usually present in a less pristine form than the fused quartz samples employed in this work. However, we begin our studies on the interaction of pharmaceuticals with mineral oxide/water interfaces by using a simple heterogeneous system whose chemical complexity can be subsequently expanded.[32,59,67] Our previous work on the interaction of Cr(VI) with such interfaces[32,58,59,67] shows that this approach is complementary to traditional soil-transport measurements, and that it provides detailed information on the molecular origin of pollutant−soil interactions. Future work will focus on tracking morantel at fused quartz/water interfaces functionalized with organic groups that are commonly found at mineral/water interfaces, such as carboxylic acids and esters.

The binding behavior of morantel citrate (Sigma, used as received) to fused quartz/water interfaces was studied directly using resonantly enhanced surface second harmonic generation (SHG). Fused quartz hemispheres (ISP optics) were housed in a custom-built Teflon flow cell as in the setup described recently.[57,58] The sample solutions pass from the reservoirs across the interface using pumps with variable flow rate controllers at 1−5 mL/s. By using a dual pump flow setup, the solute concentrations were varied in real-time. Proper mixing was ensured using a length of tubing before the sample.[58] Teflon on−off valves were used to start and stop flows. Bulk concentrations were recorded in real-time via UV−vis detection simultaneously with the surface measurements. The pH of the morantel solution and water was held at pH 7 using standard solutions of NaOH and HCl (Fisher).

III. Results and Discussion

1. Surface Spectroscopy: Figure 2 shows the SHG spectrum of morantel citrate adsorbed at the fused quartz/water interface (filled circles). The bulk solution was maintained at pH 7. The spectrum was taken at bulk concentrations resulting in monolayer coverage, as determined by adsorption isotherm measurements (vide infra). The spectral acquisition was carried out by recording the SHG intensity at a particular wavelength for 5 min. The probe wavelength was then changed by 4 nm, and

(78) Hommel, E. L.; Ma, G.; Allen, H. C. *Anal. Sci.* **2001**, *17*, 1325.
(79) Watry, M. R.; Brown, M. G.; Richmond, G. L. *Appl. Spectrosc.* **2001**, *55*, 321A.
(80) Esenturk, O.; Walker, R. A. *J. Phys. Chem. B* **2004**, *108*, 10631.
(81) Voges, A. B.; Al-Abadleh, H. A.; Musorrafiti, M. J.; Bertin, P. A.; Nguyen, S. T.; Geiger, F. M. *J. Phys. Chem. B* **2004**, *108*, 18675.

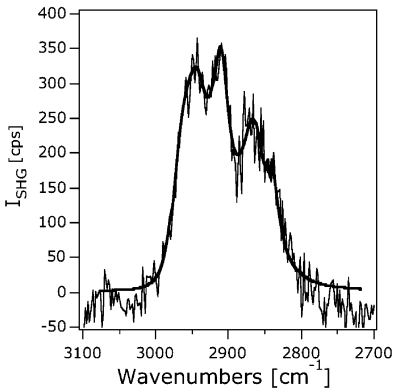

Figure 3. Broadband vibrational sum frequency spectrum of morantel deposited on a glass slide by dipping the glass slide into a 5.6×10^{-5} M morantel solution (pH 7) followed by drying (thin line) and fit of eqs 4 and 5 (thick line) with five vibrational modes. See text for details.

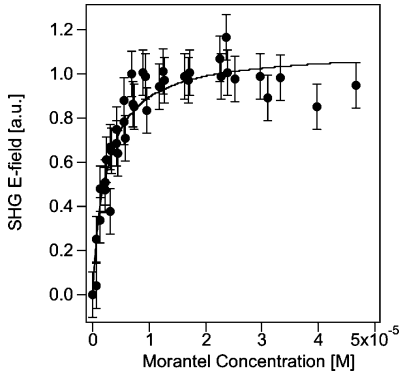

Figure 4. Isotherm for morantel adsorption at the silica/water interface maintained at pH 7 and room temperature (filled circles). The solid line is a fit to the Langmuir adsorption model according to $\theta = KC/(1 + KC)$, where θ is the relative surface coverage, K is the equilibrium adsorption constant, and C is the morantel concentration in solution.

the data acquisition process was repeated. The total spectrum was recorded in increasing and decreasing SHG wavelength steps of 2 nm over a time period of 6 h. Figure 2 shows that the SHG spectrum of morantel tracks the bulk UV−vis absorbance over the wavelength range investigated here, having a similar peak position as the bulk solution spectrum. This suggests that the n−π* transitions, which are presumably responsible for the SHG signal resonance enhancement, are not significantly perturbed when morantel is adsorbed at the silica/water interface.

To further support the notion that morantel is indeed adsorbed at the interface and to spectroscopically identify it in the CH stretching region, we measured the vibrational SFG spectrum of morantel on a glass slide that had been dipped into an aqueous morantel solution. The vibrational SFG spectrum (Figure 3, ssp polarization combination) is the average of six background-corrected 10 min broadband SFG spectra. Different spots and sample slides showed different relative intensities; however, the peak positions of the three spectral features are consistent. These features are centered near 2950, 2910, and 2875 cm^{-1}, with a shoulder at 2835 cm^{-1} and a possible second shoulder at 2975 cm^{-1}. In the CH stretching region, symmetric stretches and Fermi resonances are typically in phase with one another, but are out of phase with respect to the asymmetric stretches.[72,82,83] In addition, for a given phase, methyl CH stretches tend to be higher in frequency than methylene CH stretches.[72,82,83] The spectrum in Figure 3 is interpreted by fitting eqs 4 and 5 to the data with five vibrational modes. The fit results in the following peak positions: 2969 (5), 2939 (8), 2910 (3), 2861 (4), and 2842 (1) cm^{-1}. Referenced to the phase of the nonresonant $\chi^{(2)}_{NR}$ contribution (arbitrarily set to zero), the modes at 2969 and 2910 cm^{-1} are roughly out of phase with respect to the remaining three. This is consistent with the notion that the modes at 2969 and 2910 cm^{-1} originate from asymmetric CH_3 stretches and CH_2 stretches, respectively. Consistent with literature values on hydrocarbon systems,[72,82,83] the 2939 cm^{-1} mode is attributed to a Fermi resonance between the CH_3 symmetric stretch and a CH_3 bending overtone. Likewise, the 2861 cm^{-1} mode is attributed to CH_3 symmetric stretch, and the 2842 cm^{-1} mode is attributed to the CH_2 symmetric stretch. SFG signal intensities at and below 2800 cm^{-1} could be indicative of C−H stretches from the N−CH_3 moiety.[84] Finally, the vinylic C−H and the N−H stretches (>3000 cm^{-1}) are not observed at this IR center probe frequency. This is in contrast to the linear FTIR and Raman spectra, obtained using a BioRad FTS-60 instrument at 1 cm^{-1} and a BioRad FT Raman instrument at 2 cm^{-1} resolution, respectively (not shown). However, between 3000 and 2800 cm^{-1}, the FTIR and Raman spectral peak positions of morantel citrate are in qualitative agreement with those found using vibrational SFG.

2. Adsorption Isotherm: To assess the energetics of interaction between morantel and the fused quartz/water interface, the adsorption isotherm of morantel at room temperature was recorded (Figure 4). In these experiments, morantel binding to the interface was tracked at an SHG wavelength of 290 nm. After recording the SHG background signal from the neat interface while flowing bulk water maintained at pH 7 across the interface (no morantel present), the analyte solution (pH 7) flow was turned on using a Teflon on−off valve. The SHG signal increased, consistent with morantel adsorption and SHG resonance enhancement, and remained at a constant level once steady-state conditions with respect to adsorption and desorption were reached. This equilibrium SHG signal was then taken to represent the relative equilibrium surface coverage at the analyte concentration at which the experiment was carried out. The analyte solution flow was then turned off while flowing bulk water maintained at pH 7 across the interface (no morantel present). The SHG signal decreased, consistent with morantel desorption from the interface. After the completion of each adsorption/desorption cycle, the morantel concentration in the reservoir was increased and the experiment was repeated. The concentration of the analyte solution in a typical experiment ranged from 6×10^{-7} to 5×10^{-5} M, thereby covering the lowest detectable limit set by the USDA FSIS (0.25 ppm, or 1×10^{-6} M, referenced to 1 L of water).[26] The adsorption isotherms were recorded by starting with the lowest concentration. Figure 4 shows the adsorption isotherm of morantel citrate at the fused quartz/water interface at a pH of 7 and room temperature. It can be seen that the morantel surface coverage approaches the monolayer regime at a bulk concentration of about 1×10^{-5} M, and that the isotherm appears Langmuirian.

(82) Chen, C. Y.; Even, M. A.; Wang, J.; Chen, Z. *Macromolecules* **2002**, *35*, 9130.
(83) Opdahl, A.; Phillips, R. A.; Somorjai, G. A. *J. Phys. Chem. B* **2002**, *106*, 5212.
(84) Hesse, M.; Meier, H.; Zeeh, B. *Spektroskopische Methoden in der Organischen Chemie*, 4th ed.; G. Thieme: Stuttgart, New York, 1991.

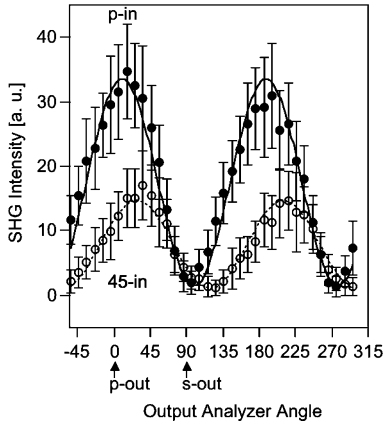

Figure 5. SHG signal intensity as a function of polarizer analyzer angle in the presence of a monolayer of morantel adsorbed at the silica/water interface. The filled circles represent the SHG polarization response while probing with p-polarized input light, and the empty circles represent the SHG polarization response while probing with 45-polarized input light.

Fitting the Langmuir model to the data results in an equilibrium binding constant, K, of $2.3(3) \times 10^7$, again referenced to the molarity of the aqueous solution under standard conditions (55.5 M).[32] At 300 K, the standard free energy of adsorption, $\Delta G°_{ads}$, is found to be 42(3) kJ/mol. This free energy is indicative of hydrogen bonding interactions between the morantel and the fused quartz/water interface. This interaction is likely to be mediated by the nitrogen centers and/or the sulfur center in morantel.

3. Orientation Studies: As shown in eq 2, adsorption isotherms measured by SHG can be influenced by number density and by orientation of the adsorbates. To test for orientational changes with increasing morantel surface coverage, we performed polarization-resolved SHG measurements. SHG studies aimed at tracking changes in the orientation of the adsorbed morantel species were carried out at a monolayer and submonolayer surface coverages of morantel, as determined by the adsorption isotherm. Two kinds of polarization studies were carried out, one in which the polarization plane of the fundamental excitation frequency at 640 nm was oriented at a 0° angle (p-in), and one in which the input polarization was chosen to be at a 45° angle (45-in) from the plane of incidence. In both sets of experiments, the SHG signal intensity was recorded at 320 nm as a function of the polarizer−analyzer angle on the output side.

The results of these polarization measurements are shown in Figure 5 for monolayer morantel coverage. As expected, the p-in/p-out polarization combination is strongest, and the p-in/s-out polarization response, which is allowed for chiral systems but not for achiral interfaces,[66] exhibits a zero-intensity SHG response within experimental error, which is consistent with the fact that morantel citrate is nonchiral. This result is also obtained for submonolayer surface coverages.

When probing a monolayer of morantel with the 45-in polarization, the SHG response of the interface is lowest at a polarizer−analyzer angle near 120°. For this input polarization, the null angle[85] does not change for submonolayer surface coverages of morantel, indicating little or no orientational rearrangement of the adsorbate with changing surface coverage. In addition, the ratio of the SHG signal intensity for the 45-in/p-out and the 45-in/s-out polarization combinations is approximately 4, indicating an approximately 4-fold stronger SHG response of morantel along the surface normal than along the interface. If the conjugated π-electron system in morantel can be viewed as the main pathway for movement of electrons that give rise to the nonlinear optical response, then morantel can be considered a rodlike chromophore. Our polarization measurements are then consistent with the notion that the conjugated π-electron system in morantel is slightly tilted away from the surface normal when it is adsorbed at the silica/water interface. Following the literature,[66,68−70,85] we calculated an orientation parameter D between 0.5 and 0.66 for angles of incidence between 45 and 55 degrees. This parameter is given the orientational average of $\cos^3(\theta)$ divided by the orientational average of $\cos(\theta)$, where θ is the molecular tilt angle with respect to the surface normal. Assuming a delta function for the orientational distribution of the adsorbed morantel would result in tilt angles between 36 and 45°, however, the angle distribution is likely to be broader, and this broader distribution would result in tilt angles larger than 43°. The orientational measurements presented here suggest that morantel is adsorbed in a tilted configuration that would allow its two nitrogen centers to interact with adsorption sites at the fused quartz/water interface through hydrogen bonding. This is consistent with the free adsorption energy of 42(3) kJ/mol derived from the adsorption isotherm measurements.

IV. Possible Environmental Implications

The equilibrium binding constant derived from our SHG adsorption isotherm measurements can be used to assess the mobility of morantel in silica-rich soil environments. To this end, we applied our data to the K_d model,[29] which is commonly used for predicting the degree to which pollutant transport is slowed due to heterogeneous binding events occurring at mineral/water interfaces. The retardation factor, R, is given by $R = 1 + (\rho/n)K_d$, where ρ is the soil density and n is its porosity. After appropriate variable transformation of the equilibrium constant to the K_d parameter,[32,58] the retardation of morantel is calculated to be 2−5% with respect to groundwater flowing through soils when using typical ρ/n ratios between 4 and 10.[31] To test this predicted high mobility of morantel, we tracked its adsorption and desorption behavior directly and in real-time at the fused quartz/water interface. Figure 6 shows that this interaction is reversible, which confirms the high mobility in silica-rich soil environments that is predicted by the K_d model when using our interface-specific binding constants. In these experiments, the SHG signal was recorded from the plain fused quartz/water interface first as a baseline reading (no morantel present). Then the morantel flow was initiated. Consistent with resonance enhancement due to the presence of the adsorbate at the interface, the SHG E-field increased until steady-state conditions with respect to adsorption and desorption were met. The morantel flow was then turned off again while flowing plain water (no morantel present), upon which the SHG E-field decreased, consistent with desorption of the adsorbate from the interface.

Figure 6 also shows that it is possible to obtain kinetic information from the SHG versus time traces. Such information is not only attainable for morantel surface coverages that are in the monolayer regime but also for submonolayer surface

(85) Hicks, J. M.; Kemnitz, K.; Eisenthal, K. B.; Heinz, T. F. *J. Phys. Chem.* **1986**, *90*, 560.

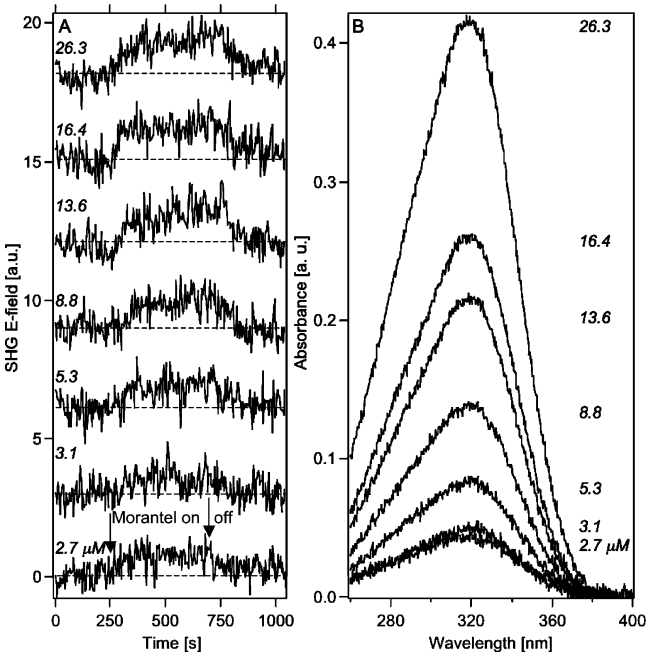

Figure 6. (A) SHG *E*-field versus time trace recorded while turning the morantel flow on and off while flowing background aqueous solution. The morantel concentrations are given in italics. The horizontal dashed lines indicate the baseline level. (B) UV−vis absorbance of morantel at concentrations corresponding to the on−off experiments.

coverages. Adsorption and desorption rate constants, together with the equilibrium constant for adsorption, can be included in chemical transport models for accurately predicting and effectively controlling the mobility of agricultural pharmaceuticals in soil environments and for assessing the fate of these contaminants under varying concentration conditions. Given the low retardation factor calculated from the measured adsorption isotherms, it is highly likely that morantel and related pharmaceuticals, such as the antibiotic pyrantel, can leach into the groundwater during raining events and possibly into municipal water systems. At their low concentrations, it is difficult to remove these compounds in water treatment plants, which suggests a low but constant background concentration of pharmaceuticals in municipal water systems. Daily intake of such water over long periods of time could thus lead to adverse health effects in humans, especially in farming communities. Future work will focus on the pH dependence of morantel binding, as well as kinetic measurements of morantel adsorption and desorption. Having demonstrated our capability to monitor these compounds at fused quartz/water interfaces, we plan to study related pharmaceuticals as well, from which structure−mobility relationships may be developed.

V. Summary

In conclusion, the results presented in this work are the first direct, interface-specific studies that address the mobility of a widely used agricultural pharmaceutical, namely, morantel, which is commonly present in farm runoff. The measurements are carried out using nonlinear optical laser spectroscopy and allow us to study the interaction of morantel with fused quartz/water interfaces in the micromolar to submicromolar concentration regime. We identified the adsorbed compound via the two-photon resonance of its n−π* transition and its vibrational features in the C−H stretching region, and measured a free energy of adsorption to the silica/water interface of 42(3) kJ/mol at pH 7. This work shows that the ability to track monolayer and submonolayer amounts of pharmaceuticals at solid/liquid interfaces is key to assessing their mobility in the environment. While such surface-specific studies are, in principle, possible with ATR−FTIR or Raman-based spectroscopies, SHG provides the sensitivity and the real-time capability necessary for making such assessments. We find that the interaction of morantel with fused quartz/water interfaces is fully reversible, indicating a high mobility in silica-rich soil environments. This high mobility could lead to an increased interaction of morantel with target organisms, which could respond by increasing their drug resistance. Furthermore, this work indicates that pharmaceuticals discharged into the environment could enter the groundwater supply of municipal water systems, at which point their removal is challenging. Future work will address the pH dependence of morantel interaction with the mineral/water interface.

Acknowledgment. The authors gratefully acknowledge helpful comments by two anonymous reviewers. We also acknowledge donations and the technical support of Spectra Physics and CVI Lasers. A.B.V. acknowledges a NASA Graduate Student Fellowship in Earth Systems Sciences (NGT-530456). Financial support for this work was provided by the NSF (CAREER Award CHE-0348873), the ACS-PRF (Grant 38960-G5S), the Northwestern Institute for Environmental Catalysis (CHE-9810378 and DE-FG02-03-ER15457), and Shell Oil Company.

JA054837B